

Bulletin of the Seismological Society of America

Vol. 67

June 1977

No. 3

STRONG-MOTION RECORDINGS OF THE CALIFORNIA EARTHQUAKE OF APRIL 18, 1906

BY DAVID M. BOORE

ABSTRACT

Recordings from a low magnification ($V = 4$), intermediate period ($T \approx 5$ sec) seismograph at Mt. Hamilton, within 35 km of the San Andreas fault, show about 8 sec of P -wave energy and the first half-cycle or so of the initial S wave before going off-scale. The times, polarities, and overall amplitudes are consistent with Bolt's conclusion (1968) that the main shock began closer to San Francisco than Olema, as originally proposed by Reid (1910). This and the distribution of surface slip imply a bilateral rupture, but the seismic moment for the segment to the northwest was on the order of 2.5 times greater than for the southeasterly segment. Although Mt. Hamilton is only 35 km from the rupture surface, the most massive faulting apparently took place at least 75 km away. The recording at Mt. Hamilton returned to scale after about 60 sec; the duration of energy with periods close to 5 sec was comparable to that from more recent strong-motion recordings.

Theoretical modeling using both body and surface waves showed that the surface waves dominated the motion at Mt. Hamilton. The modeling also emphasized the sensitivity of the ground motion to directivity effects and rupture velocity. The general characteristics of the data (polarity, amplitude, period content, and duration) were matched reasonably well by a simple dislocation model using fault lengths, depths, and offsets determined from independent data.

INTRODUCTION

Standard catalogs of strong-motion data contain no listings of records of great earthquakes at distances within several hundred kilometers of the faulting. Such data are critical to the earthquake engineering design of important facilities, and lacking such data a number of theoretical, empirical, or intuitive methods have been used to generate design motions. Considering the obvious need to check the reliability of these motions, it is surprising that strong-motion recordings within 50 km of the faulting in two $M > 8$ earthquakes have been generally ignored by seismologists and engineers. These earthquakes are the 1923 Kanto earthquake, recorded at Tokyo within about 35 km of the faulting (Kanamori, 1974), and the April 18, 1906, California earthquake, recorded at the Lick Observatory on Mt. Hamilton (Figure 1). The latter recordings are readily available in the Atlas accompanying the classic *Report of the State Earthquake Commission* (A. C. Lawson, Chairman), referred to hereafter as the *Report*. (The two volumes of the *Report* and the Atlas were reprinted in 1969 and can be obtained from Academic Press under the title *The California Earthquake of April 18, 1906* for \$22.50, as of March, 1976). The neglect of these records is probably due both to the loss of the peak motions and to the intermediate periods (around 5 sec) of the on-scale motions. Considering the lack of any other close-in

recordings from great earthquakes, however, the records are important in spite of their limitations. Indeed, engineering structures such as offshore drilling platforms, bridges, storage tanks and tall buildings have resonant periods of several seconds, in the range recorded by the instruments. The loss of the peak motions is regrettable, but the records can be used to estimate duration of strong shaking (as was done by Bolt, 1973), to aid in the location of the earthquake epicenter (Reid, 1910, Vol. II of

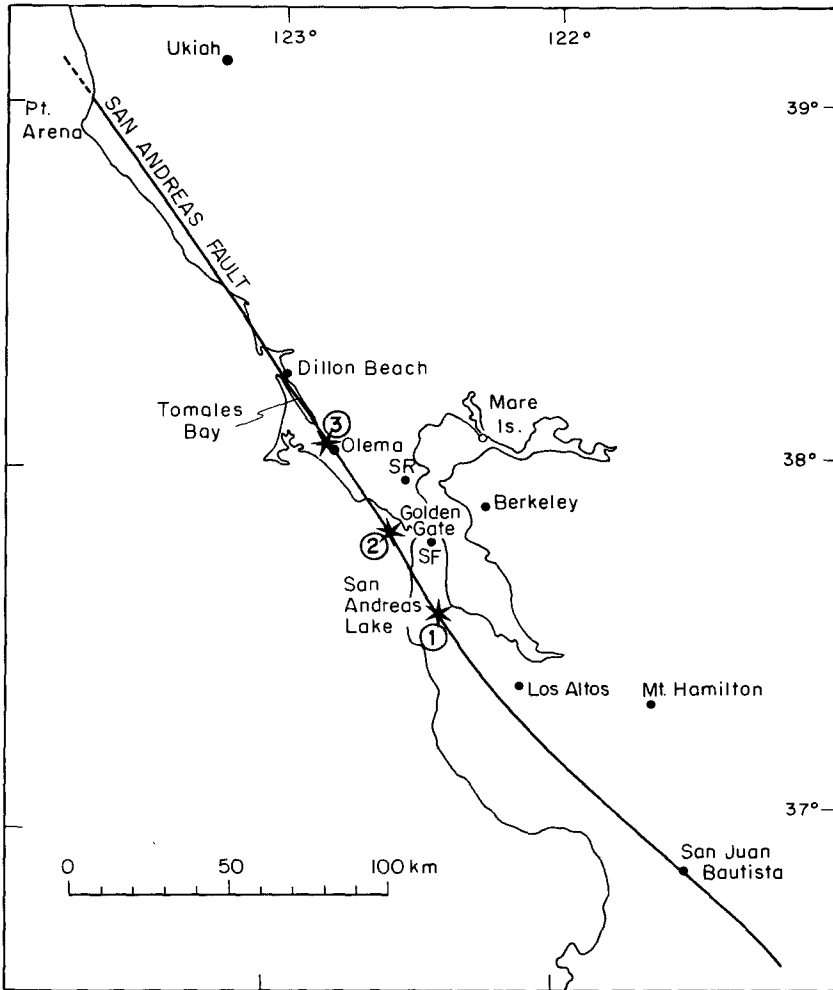


FIG. 1. Location map, showing the San Andreas fault and the epicenters used in the dislocation modeling (stars). SF and SR stand for San Francisco and San Rafael.

the *Report*, and Bolt, 1968, for the 1906 record), to check techniques for the synthesis of strong ground motion, and to derive source parameters of great earthquakes (see Kanamori, 1974 for such a use of the 1923 record).

In this paper we reinterpret the epicenter location, using a different identification of phases than in previous work, and then use this location and independently determined faulting parameters to compute the ground motion at Mt. Hamilton, including both body and surface waves. The overall characteristics of the observed recordings are matched by the theoretical motions. As will be seen, most of the information in the records pertains to the rupture southeast of the epicenter, although the majority of

the faulting was to the northwest. Ben-Menahem and Kovach (personal communication, 1976) have used teleseismic surface waves to extract information about the northwestern part of the rupture.

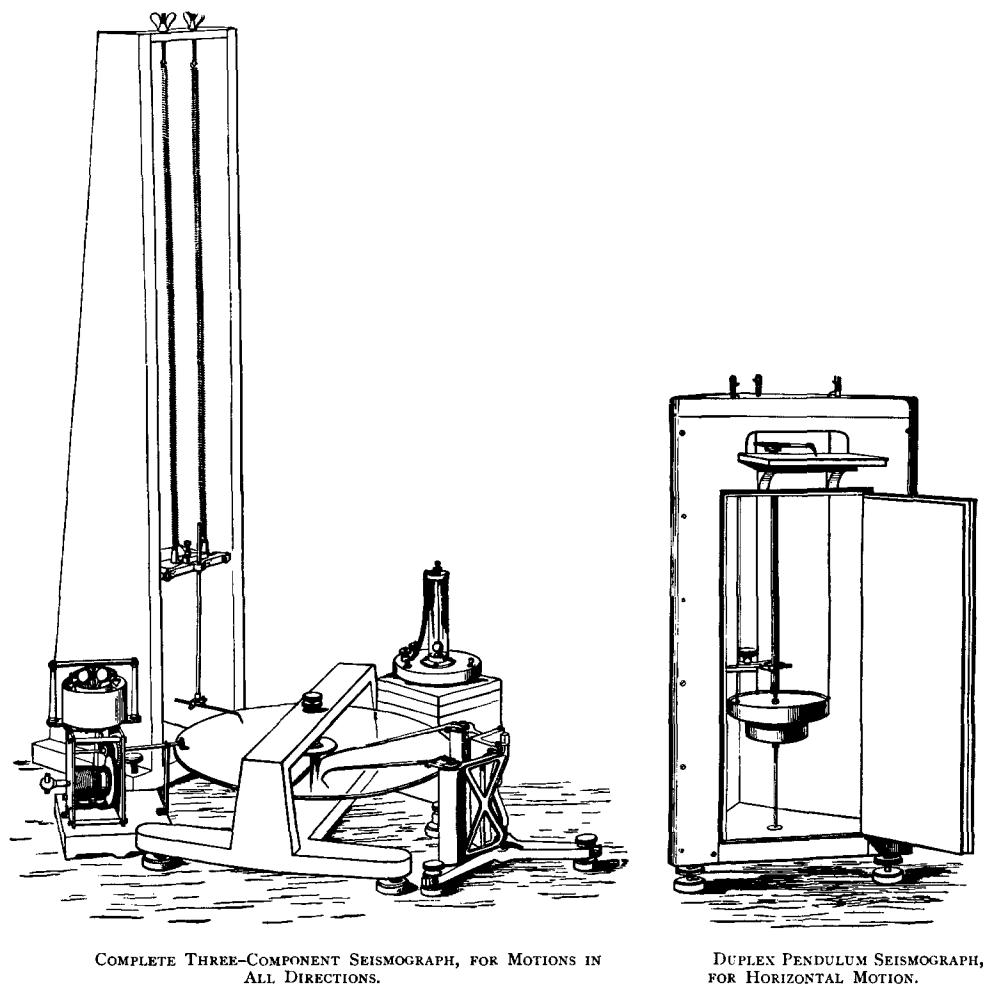


Fig. 2. The Ewing seismographs which recorded the 1906 earthquake at Berkeley and Mt. Hamilton (from Holden, 1887; also see Ewing, 1886).

THE RECORDINGS

Instruments. Of the eight California records published in the Atlas (see plate 29 of the Atlas), three are uncluttered enough to be of some use in determining fault parameters. These were recorded at Berkeley and Mt. Hamilton on instruments designed by J. A. Ewing (see Figure 1 for location, and Louderback, 1942, for details of their acquisition). Both stations had a duplex pendulum and a three-component seismograph (Figure 2), but the latter instrument did not provide a record at Berkeley. The instruments are described by Ewing (1886) and Dewey and Byerly (1969).

The duplex instrument (Figure 2, *right*) provided records similar to those from the strong-motion seismoscopes used today (Cloud and Hudson, 1961). A pen traced the two-dimensional horizontal movement of the pendulum on a smoked-glass plate and

no timing information was provided. The three-component system (Figure 2, *left*) used a horizontal pendulum to trigger the rotation of a circular smoked plate. The motions of two horizontal pendulums were recorded on the plate. A clock, not shown in Figure 2, was also started and put time marks on the edge of the plate.

No mention of instrumental free periods or dampings could be found in Ewing's

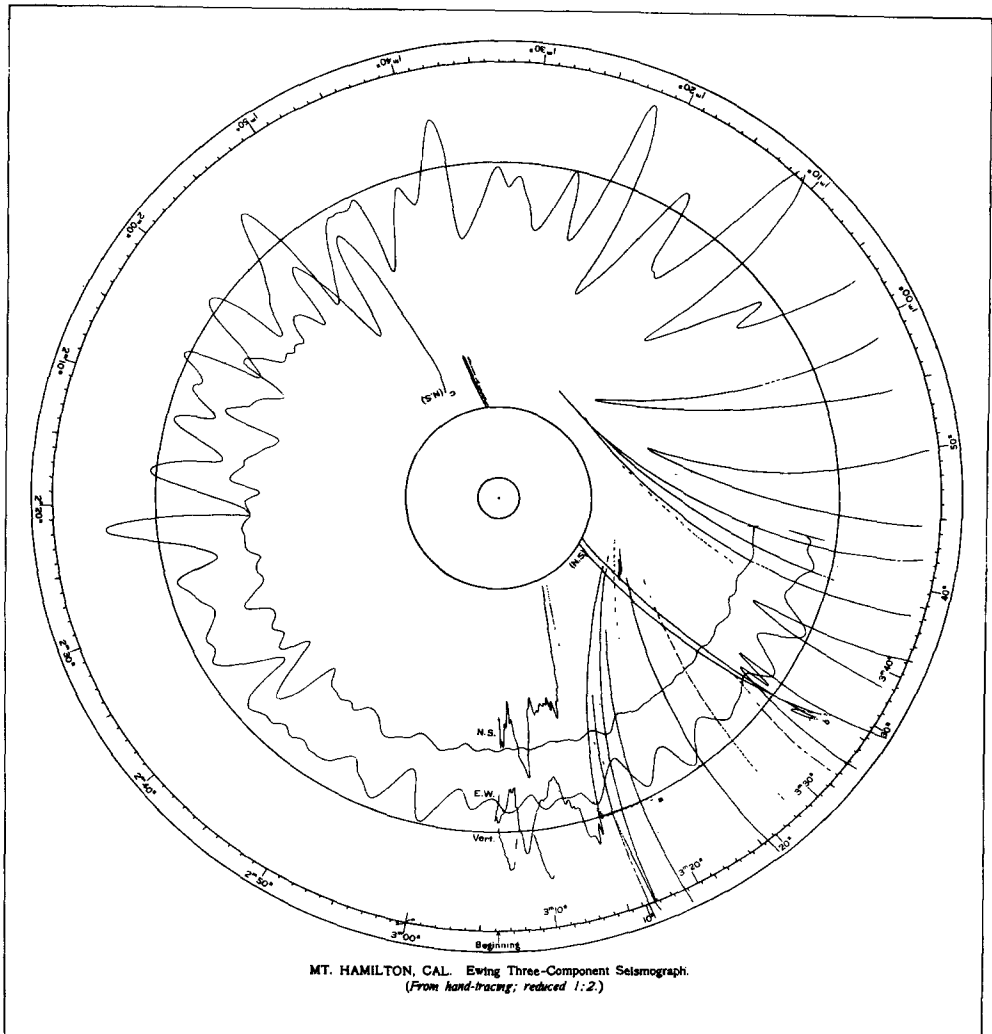


FIG. 3a. The Ewing three-component seismograph record from Lick Observatory, Mt. Hamilton (from plate 29 of the Atlas accompanying the *Report*.) See Figure 3b for the amplitude scale.

publications (e.g., 1881, 1884a, b, 1885, 1886, 1887). He called the general design of the three-component system an "Astatic Horizontal Lever Seismograph" (Ewing, 1881), and it is clear that the free period was of little importance so long as it was greater than the period of ground motion. We have assumed the free period of the Mt. Hamilton instrument to be 5 sec, close to the dominant period in the record. Unfortunately the Mt. Hamilton instrument cannot be found (McEvelly, personal communication, 1976) so we cannot test our assumption directly. The free period of 5 sec, however, gave a better fit of the theoretical *P* waves to the data than did free periods of 2.5

or 10.0 sec. Damping was provided by friction at the hinges and between the stylus and plate. This was arbitrarily taken as 20 per cent in subsequent calculations; the results are not overly sensitive to this parameter.

Records. The three-component seismograph record is shown in Figure 3. Although off-scale during much of the strongest shaking, enough character is present to be of some use in determining fault parameters. To provide a more conventional display, a manual process was used to straighten the time axis and to compensate for the finite radii of the pen deflections (Figure 3b). The vertical component went off-scale soon after triggering and will not be considered further. The pendula were quite stable, as shown by the return of the pens to positions close to the starting position (this is especially true of the EW motion; a noticeable offset occurred in the starting and stopping positions of the NS pen). In spite of this stability, the relative vertical positions of the unwrapped motions between 10 and 40 sec may be uncertain. In particular,

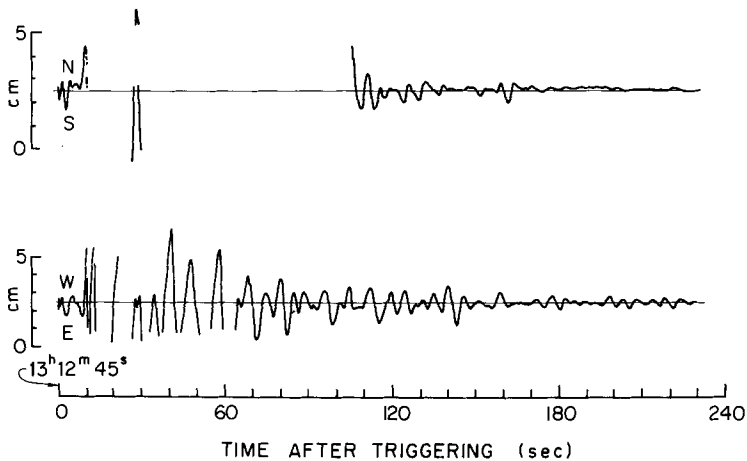


FIG. 3b. The unwrapped seismograms. The amplitudes have been normalized by the static magnification of the instrument. The component orientations indicate the direction of ground motion.

the EW motions between 25 and 35 sec are suspect. They have been included to show that some motion was recorded on the plate, but no guarantee of the vertical position is made.

The time scale at the beginning of the record may be somewhat uncertain because, although the plate should take a few seconds to attain normal speed after triggering (Ewing, 1887, p. 107), the time marks on the rim as the record appears in the Atlas are evenly spaced. This inconsistency may be the result of a draftsman's overzealous efforts at tidying up the copy of the record which appears in the Atlas. We can only hope that he used the time marks on the original as a guide.

The duplex pendulum records from Mt. Hamilton and Berkeley are shown in Figure 4. The motions are strongly influenced by the stops limiting the motion of the pendulum, but the initial part of the motion is clear. Again, no mention of free period or damping of this instrument could be found.

The question of polarity. Although not explicitly shown on the three-component record (Figure 3a), the labeling of components in Figure 3b has been inferred from Reid (1910, pp. 64 and 65), who stated that the first motion was to the southeast, followed about 9 sec later by the strong motion directed toward the northwest. If, as

argued later, the instrument was triggered soon after the P arrival, if the strong motion represents S energy, and if the epicenter was on the fault to the northwest of Mt. Hamilton, we run into an apparent inconsistency at first glance. A simple right-lateral double-couple model would predict initial S motion to the northeast, not north-

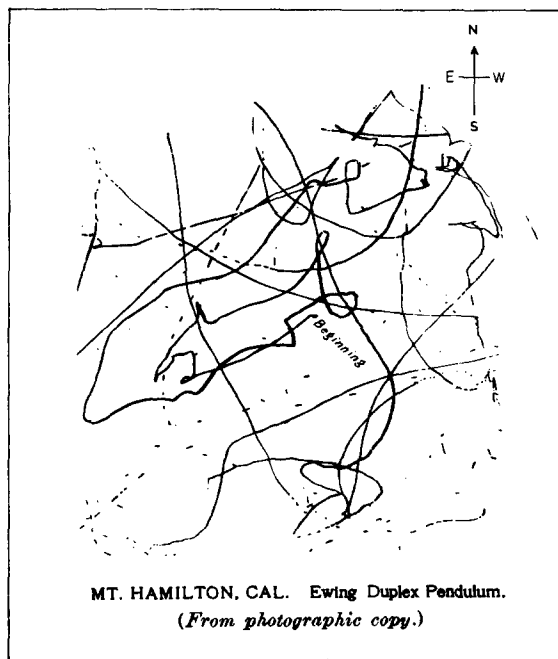
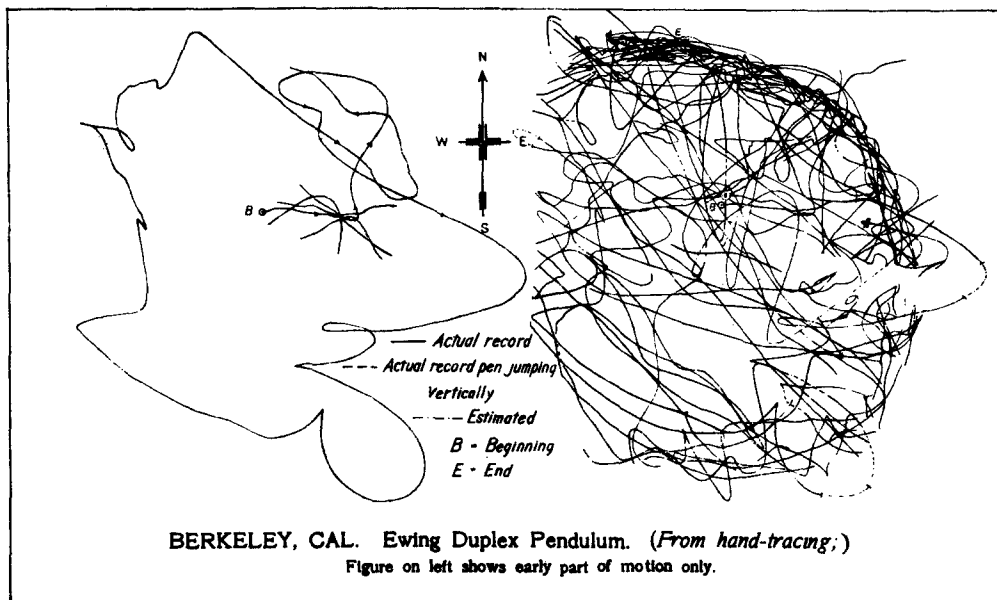


FIG. 4. The duplex pendulum records at Mt. Hamilton and Berkeley. See Figure 5 for the amplitude scale. Compass bearings give the direction of ground motion (modified from plate 29 of the Atlas accompanying the *Report*; E and W on the Mt. Hamilton record have been interchanged on the basis of Reid, 1910, p. 64).

west. Reid recognized this difficulty (Reid, 1910, p. 113). In fact, careful inspection of the record shows that the onset of strong motion is almost 2 sec earlier on the NS trace than on the EW trace, and it seems to correlate with a small but definite eastward motion. Furthermore, the dislocation modeling suggests that the initial *S* motion should be smaller on the EW trace than on the NS trace. Thus, in spite of first appearances, the polarities shown on Figure 3b are consistent with the expected northeastward direction of initial *S* motion.

Another check on the consistency of the polarities is given by comparing the particle motion plot obtained from the first 9 sec of the NS and EW three-component traces with the initial movements of the duplex pendulum record (Figure 5). The comparison is quite good, considering that the instruments are probably not matched and that the initiation time of the duplex pendulum record is not known.

REEVALUATION OF EPICENTERS

Previous work. Reid (1910) used times of felt motions at San Francisco, Berkeley, Mt. Hamilton, and Ukiah to locate what he referred to as the "beginning of the shock"

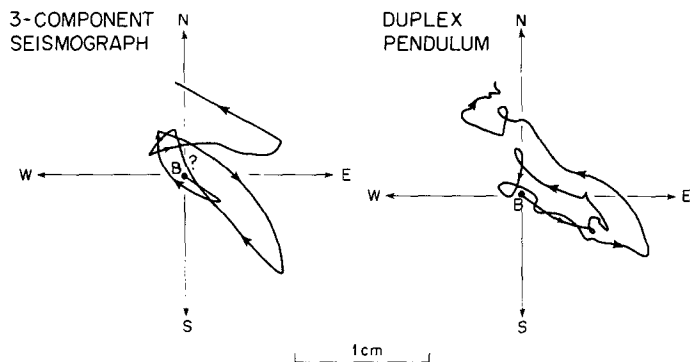


Fig. 5. Ground motions in the horizontal plane. The beginning of the motion from the three-component seismograph is uncertain. The amplitudes have been normalized by the static magnification of the instrument. The rectilinear NW-SE motion is interpreted as *P* waves from an epicenter to the northwest along the San Andreas fault.

off the Golden Gate (epicenter 2 in Figure 1). Reid (1910) and Bolt (1968) showed that this was a foreshock, followed by the main shock (Reid's "violent shock") which Reid located near Olema (epicenter 3 in Figure 1) using times at which clocks stopped at San Rafael, Mare Island, and Berkeley and the trigger time of the Mt. Hamilton instrument. Bolt (1968) reinterpreted the main-shock location using teleseismic data as well as Reid's times, and found a preferred solution between epicenters 1 and 2 in Figure 1.

Foreshock. Although this paper is concerned primarily with the records from the main shock, it should be pointed out that the location of the foreshock, which was based entirely on felt times, is quite uncertain. Even assuming that the clocks were accurate, it is not clear what phase of ground motion was felt by the observers. Reid (1910) and Bolt (1968) assumed it was the *P* wave. On the other hand, the Ukiah time was estimated by Prof. Townley, who "... had been at work very late the previous night and was sleeping soundly when he was awakened by the earthquake" (Reid, 1910, p. 5). Although the soundness of one's sleep is difficult to quantify, it is unlikely that Townley was awakened by the *P* waves of a foreshock over 150 km away. If we make the assumption that he was awakened by the *S* waves, an epicenter

close to Dillon Beach near the mouth of Tomales Bay (Figure 1) gives a good solution (Table 1). Because of the uncertainties in the type of felt motion, however, little reliance should be placed on any of the foreshock locations.

Main shock. Fortunately, the record from the Ewing three-component seismograph at Mt. Hamilton allows us to be more definite about the location of the main shock. We assume on the basis of polarizations, dislocation modeling, and comparisons with records at similar distances from more recent, but smaller, earthquakes that the instrument was triggered by *P* motion and that the strong arrival on the NS component at about 8 sec after triggering corresponds to the *S* arrival. This differs from Bolt (1968), who identified the *S* wave with the triggering of the instrument and the later

TABLE 1
TRAVEL TIMES FOR AN EPICENTER NEAR DILLON
BEACH, ASSUMING *S* ARRIVALS AT UKIAH AND *P*
ARRIVALS ELSEWHERE

Station	Δ Distance (km)	Observed Travel Time* (sec)	Calculated Travel Time† (sec)
San Francisco	68	11	12
Berkeley	75	17	13
Ukiah	103	28	30
Mt. Hamilton	153	23	24

* Origin time: 13h 11m 49s.

† Using the crustal model in Table 2.

TABLE 2
CRUSTAL MODEL FROM BOLT ET AL. (1968)

Layer Thickness (km)	Compressional Velocity (km/sec)	Shear Velocity (km/sec)
12	5.6	3.3
18	6.7	3.9
—	8.0	4.7

strong motion with a surface-wave arrival. In spite of these differences, the conclusions here are similar to Bolt's. Our interpretation gives a minimum *S* - *P* time of about 8 sec. The vertical lines at the beginning of the traces indicate that the pendulums were swinging before the plate began to revolve. This means that the actual *S* - *P* was longer than 8 sec and that the minimum epicentral distance was about 64 km, requiring that the epicenter be either along the fault to the southeast of San Juan Bautista or northwest of a point about 13 km south of San Andreas Lake. We can rule out the first possibility from, among other things, Bolt's (1968) teleseismic study and the times at which the pendulum clocks stopped.

We have an estimate not only for the *S* - *P* time, but also for the absolute arrival time of the *S* wave at Mt. Hamilton (13h 12m 53s). From this, the origin time has been computed for a number of trial epicenters, using the crustal model of Bolt *et al.* (1968, see Table 2). The results are given in Table 3. An epicenter at the minimum distance of 64 km implies an origin time which is later than both the stopping of the pendulum clock at San Rafael and the origin times determined from the teleseismic

waves, estimated by Bolt (1968) to be within several seconds of 13h 12m 21s. On the other hand, the origin time for the Olema epicenter is earlier than that inferred from the teleseismic recordings by about 5 sec. An epicenter near the Golden Gate is consistent with the origin times estimated from the Mt. Hamilton record and the teleseismic waves. This epicenter is also consistent with the cessation of clock motion at various sites (Table 4, where we have adopted Bolt's assumption that the clocks were

TABLE 3
ORIGIN AND *P* ARRIVAL TIMES INFERRED FROM AN *S* ARRIVAL AT 13H 12M 53S AT MT. HAMILTON,
FOR VARIOUS EPICENTERS

Epicenter	Distance (km)	Origin Time	<i>S</i> - <i>P</i> Time (sec)	<i>P</i> Arrival Time	<i>T</i> * - <i>P</i> Time (sec)
1. San Andreas Lake	75	13h 12m 30s	9	13h 12m 44s	1
2. Golden Gate	100	13h 12m 24s	12	13h 12m 41s	4
3. Olema	130	13h 12m 17s	15	13h 12m 38s	7

* *T* = trigger time.

TABLE 4
COMPARISON OF *S* TRAVEL TIMES AND TIME INTERVAL BETWEEN INITIATION OF RUPTURE AND THE
STOPPING OF PENDULUM CLOCKS, USING THE ORIGIN TIMES IN TABLE 3

Station	(1) San Andreas Lake			(2) Golden Gate			(3) Olema		
	Distance (km)	(<i>S</i> - <i>O</i>) (sec)	(<i>S</i> * - <i>O</i>) (sec)	Distance (km)	(<i>S</i> - <i>O</i>) (sec)	(<i>S</i> * - <i>O</i>) (sec)	Distance (km)	(<i>S</i> - <i>O</i>) (sec)	(<i>S</i> * - <i>O</i>) (sec)
San Rafael (<i>S</i> * = 13h 12m 32s)	43	13	2	17	5	8	26	8	15
Mare Island (<i>S</i> * = 13h 12m 35s)	57	17	5	42	13	11	48	15	18
Berkeley (<i>S</i> * = 13h 12m 38s)	37	11	8	32	10	14	54	16	21

* These times were used by Reid (1910) in his location of the "violent shock". They are about 1 sec earlier than the time indicated on the clocks.

stopped by *S* waves). The directions of first motion on the duplex pendulum records at Berkeley (Figure 4) and Mt. Hamilton (Figure 5) also give slight evidence for such an epicenter, assuming that the first motions are *P* waves which have not been refracted laterally.

DISLOCATION MODELING

In view of the off-scale amplitudes at Mt. Hamilton and lack of data at other stations, we cannot hope to extract much detail about the rupture process from the data. Instead, our approach was to see how well the records could be modeled using straightforward dislocation models and parameters derived from other studies. In so doing, an appreciation for the importance of rupture velocity and directivity emerged, and this led to some limited parameter studies.

We modeled both body waves and surface waves. The body waves were computed

using the Haskell formulation of Boatwright and Boore (1975). The near-field terms and rupture propagation effects are accurately accounted for in this procedure, but the model assumes that the dislocation is embedded in an infinite medium with no free surface or layering. From Anderson (1976), however, we can argue that the free surface effect is adequately accounted for by doubling the motion. The influence of crustal layering is important in a detailed comparison of observed and synthetic data, especially since refractions and wide-angle reflections from the intermediate crustal layer and the Mohorovičić discontinuity are expected within several seconds of the first arrivals. A sample calculation for a model with two half-spaces welded together, using the generalized ray theory of Helmberger (1974), suggested that in our case the overall amplitude and wave shape in the first cycle or so of motion may be similar

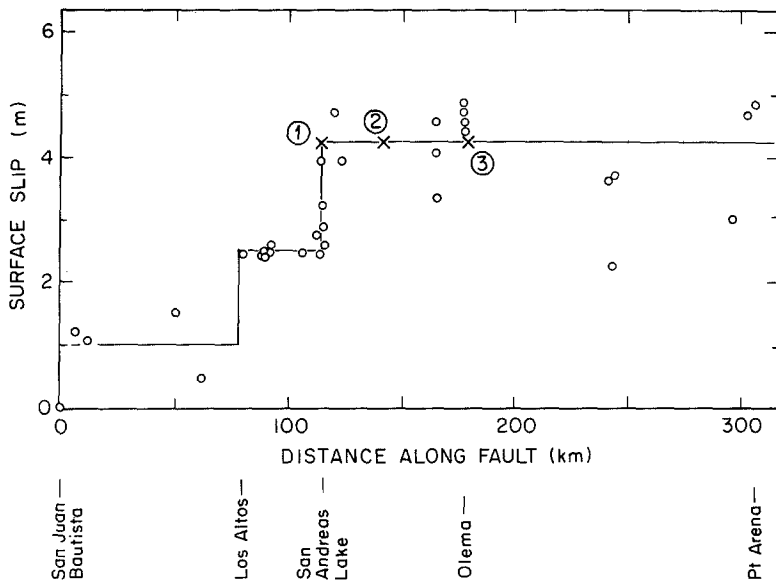


FIG. 6. The observed surface slip compiled from various sources, including the *Report* and personal field notes, by Kerry Sieh. In some instances slip values are uncertain by at least $\frac{1}{2}$ m. The lines show the location and slip for the dislocation model of the earthquake, with the assumed epicenters marked by *x*'s.

to that from the direct wave only. The amplification due to the velocity gradient near the Earth's surface may, however, increase the body-wave amplitudes by about 50 per cent over what we have calculated.

In contrast to the body-wave calculations, the surface-wave synthesis accounts for crustal layering and free-surface effects. We used the formulations of Harkrider (1970) and Ben-Menahem *et al.* (1970) with allowances for attenuation. Near-field terms were not included but are unimportant for the periods (around 5 sec) and distances (greater than 30 km) considered here. The finiteness of the source was accounted for by breaking the rupture into a number of point sources, with an appropriate directivity factor for each source (Ben-Menahem and Singh, 1972). This procedure is similar to that used by Aki (1968) and Butler *et al.* (1975). By combining the infinite media body waves and the surface waves, we account for almost all motion except that within about 5 sec of the initial body-wave arrivals.

The fault was modeled by a number of segments (three for the epicenter near San Andreas lake and four for the epicenters off the Golden Gate and near Olema) with

the total dislocation, length, and orientation of each segment consistent with the distribution of surface displacement given in the *Report* (Vol. I). Figure 6 shows the observed slip and the assumed slip on each segment. The starting time and location of initial faulting on each segment was chosen to simulate bilateral rupture from the epicenter. The width of each segment, 10 km, was taken from analysis of geodetic data (Thatcher, 1975), and the rise time of the ramp source time function was held fixed at 3 sec. Most of the results are shown for a rupture velocity of 3 km/sec.

Figure 7 shows the computed body-wave ground displacement and the corresponding instrumental record for rupture starting off the Golden Gate. Clearly, the longer-period near-field contributions, such as the static offsets and the monotonic ramp between the *P* and *S* arrivals, are largely removed by the instrument response. A computation using only far-field terms from distributed point sources gave very similar instrumental records, suggesting that the procedure used in the surface-wave synthesis,

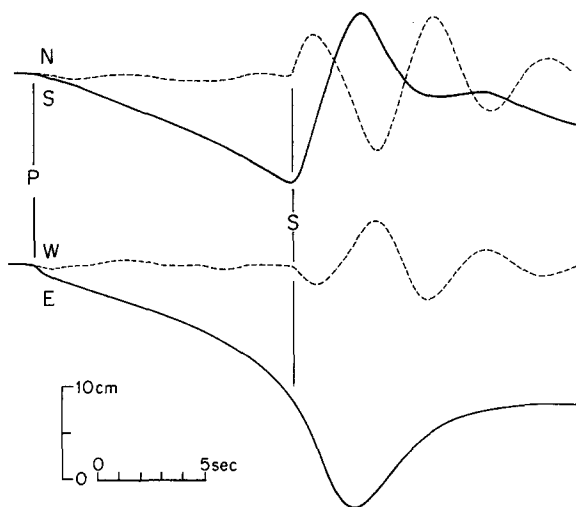


FIG. 7. Computed body-wave motion for epicenter 2 off the Golden Gate without and with the assumed instrument response (solid and dashed lines, respectively). *P* and *S* show the arrivals of the initial *P* and *S* waves from the epicenter.

which ignores near-field terms, is valid for the periods and distances of interest in this paper.

The predicted instrumental records for the three epicenters are compared with the data in Figure 8. The data and model results have been keyed to one another by assigning the initial *S* wave the arrival time 13h 12m 53s. The overall comparison is quite good; considering the assumptions and simplifications that have been made, refinements of the dislocation model are not justified. The most striking differences between the motion from the three epicenters is the ratio of the *P* and *S* motion and the absolute amplitude of the *S* motion, especially on the EW component. For example, note the change in the height of the first peak of the *S* wave on the EW component: as the epicenter moves to the south the peak is reduced in amplitude, eventually becoming no larger than the *P* motion before it. These epicenter-dependent characteristics of the computed motions, due in large part to changes in the radiation patterns, suggest that the epicenter was between San Andreas Lake and the Golden Gate.

Figure 8 also shows the results for a 2-km/sec rupture starting off the Golden Gate. The sensitivity of the *S*-wave amplitudes to rupture velocity is expected from simple

far-field considerations, which predict that the ground displacement goes as $(1/M - \cos \theta)^{-1}$, where $M = V/C$, V and C are the rupture and propagation velocities and θ is the azimuth from the fault strike to the station (Savage, 1971). The closer M^{-1} gets to $\cos \theta$, the more sensitive is the amplitude to rupture velocity. This explains

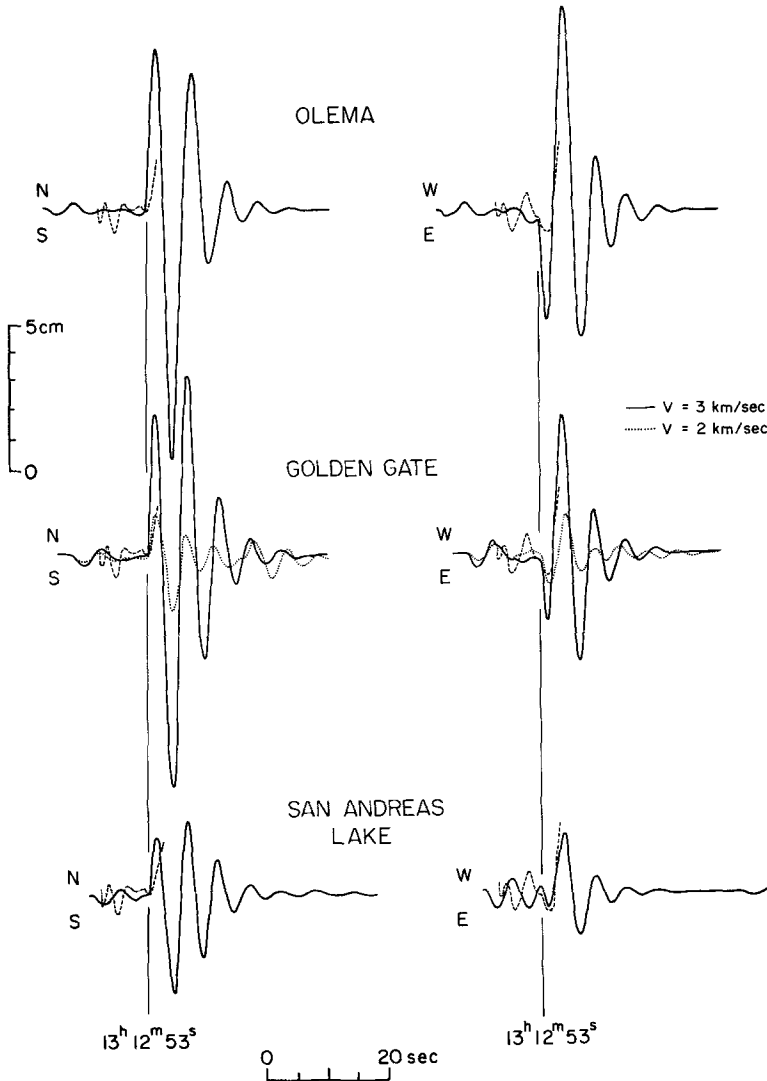


FIG. 8. Computed (solid) and observed (dashed) body-wave motions for the three epicenters.

why the P wave, with $M = 0.5$ and 0.4 shows less change than does the S wave, with $M = 0.9$ and 0.6 .

The surface-wave results, using the crustal model in Table 5, are compared with the data in Figure 9 for rupture starting off the Golden Gate. The fundamental mode motions are shown; contributions for the higher modes are negligible. By comparing Figures 8 and 9, it is clear that surface waves dominate the motion at Mt. Hamilton, even if allowance is made for local amplification of the body waves. The sensitivity to rupture velocity is even more extreme for the surface waves than for the body waves since the phase velocity for 5-sec period, 2.6 km/sec, is such that C/V is close to $\cos \theta$

for $V = 3$ km/sec (in this case the rupture propagates at a transonic speed compared with the phase velocity). Several other crustal models were used, but the basic findings above were not changed.

Although the rupture was bilateral, the theoretical motions are most sensitive to the southeast extension of faulting. This is shown in Figure 10, in which the body-

TABLE 5
CRUSTAL MODEL USED IN SURFACE-WAVE
COMPUTATIONS

Layer Thickness (km)	Shear Velocity (km/sec)	Density (gm/cc)	Q
0.3	1.0	2.0	60
1.3	1.6	2.3	100
2.2	2.9	2.6	210
12.0	3.3	2.7	300
18.0	3.9	3.0	400
—	4.7	3.3	800

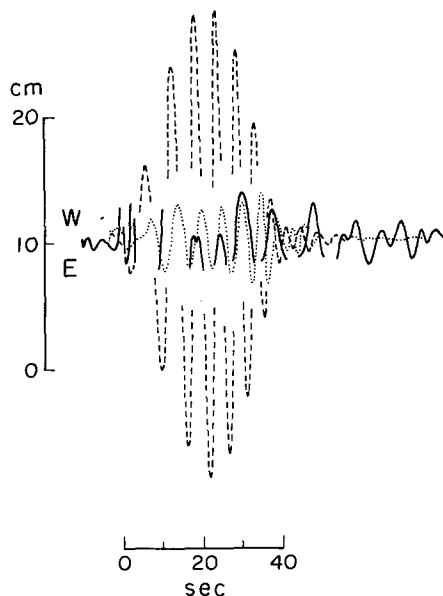


FIG. 9. Surface-wave motions for rupture velocities of 2 and 3 km/sec (dotted and dashed lines, respectively) compared with data (solid line). The theoretical motions in the north-south direction are about 65 per cent larger than the east-west motions shown here.

wave motions from the two segments adjacent to the Golden Gate epicenter are compared. The surface-wave motions give similar results. The large difference in the amplitude of the motions is a result of the directivity due to the rupture propagation; a smaller but still striking difference exists for rupture at 2 km/sec. The importance of directivity is enhanced since the azimuth between the more potent fault segments around the epicenter and Mt. Hamilton is less than 30° . In spite of the major contribution made by the southeastward rupture to the Mt. Hamilton record the average observed surface slip, and presumably the fault dislocation, is much higher to the northwest of the possible epicenters than to the southeast, and thus at teleseismic distances the directivity should show that the dominant rupture was to the northwest.

Some simulations were made using statistical variations in fault parameters, the purpose being to assess the dependence of the directivity effect on the coherence of the rupture process. It was not possible to eliminate the effect so long as rupture was nonrandom to the extent that it began at an epicenter and moved away in both directions at a predetermined mean velocity.

COMPARISON WITH STRONG-MOTION DATA

From the view of earthquake hazards, it is important to compare the Mt. Hamilton motions with strong ground motion from other large earthquakes. Although incomplete, the Mt. Hamilton seismogram is one of the two recordings to date within 100

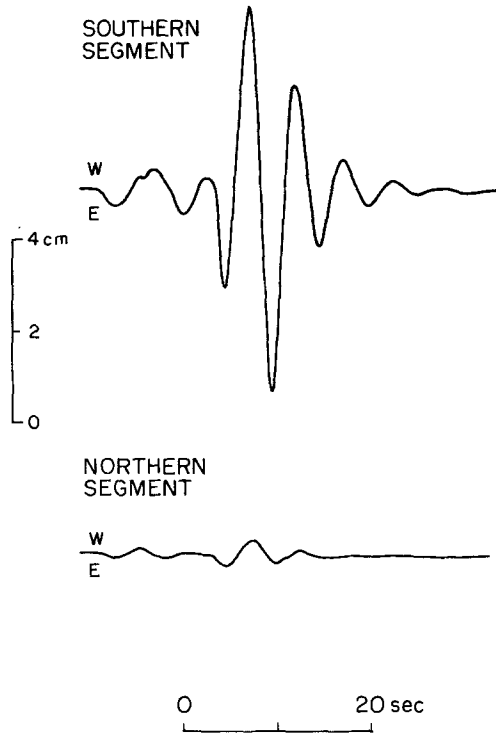


FIG. 10. Computed motions from rupture in both directions from the epicenter off the Golden Gate. The southern segment extends to the large offset in slip near the San Andreas Lake; the northern segment extends beyond Pt. Arena.

km of a magnitude 8 earthquake. The record gives a lower bound for the peak motion and can be used to determine duration of intermediate period waves (Bolt, 1973). It should be recalled, however, that although the fault surface comes within 35 km of Mt. Hamilton, the surface rupture was small here compared to the rupture farther north. The major part of the faulting apparently occurred at distances over 75 km from the station. This suggests that the ground motions would have been greater for sites to the north at comparable distances from the fault. There is slight support for this in the intensity map of the earthquake (plate 23 of the Atlas), but the effects of local geology and, possibly, sympathetic faulting complicate the picture (for example, anomalously high intensities were observed to the south of San Juan Bautista, away from the fault trace, in the Salinas River Valley and near Los Banos). There was not much damage at Mt. Hamilton; according to the *Report* (p. 306, Vol. I) "not much plaster fell and only one of a dozen or more chimneys were thrown".

In average period content the Mt. Hamilton record is similar to a displacement record obtained from the double integration of an accelerogram, and for this reason we have compared the motion with a number of displacement traces from well-known earthquakes, including the 1923 Kanto event (Figure 11). To insure a valid comparison, the displacement records were put through the instrument response assumed for

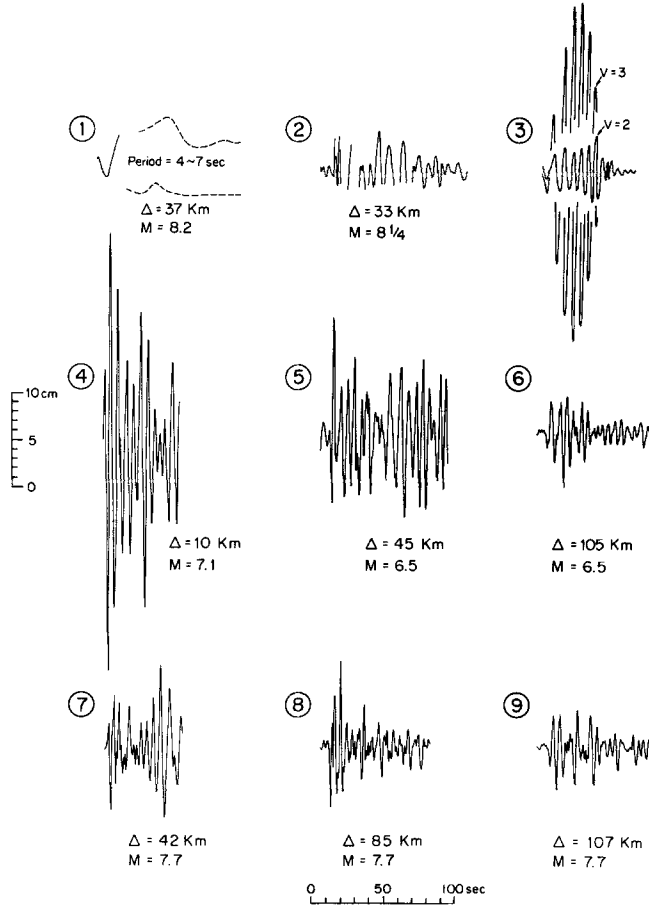


FIG. 11. Comparison of ground motions. All records except for the Kanto record (1) have been put through the assumed Mt. Hamilton instrument response. The Kanto record was normalized by the static magnification of the instrument on which it was recorded ($T = 10$ sec, damping ≈ 0.5). Δ is the closest distance of the fault surface from the station, as given by Page *et al.* (1972). The records correspond to the following earthquake, station (component) pairs: (1) 1923 Kanto at Tokyo (N37E); (2) 1906 at Mt. Hamilton (N90E); (3) surface waves from 1906 (N90W, see Fig. 9); (4) 1940 Imperial Valley at El Centro (S90W); (5) and (6) 1968 Borrego Mountain at El Centro (S00W) and San Diego (N90E); (7), (8), and (9) 1952 Kern County at Taft (S69E), Santa Barbara (S48E), and Hollywood P.E. lot (S00W). Data in (4) through (9) are from the *Strong Motion Earthquake Accelerogram* reports issued by the Earthquake Engineering Research Laboratory at California Institute of Technology.

the Mt. Hamilton recordings (free period is 5.0 sec, damping is 0.2 of critical). The general effect was to amplify the peak motions by about 25 per cent. With the exception of the 1968 El Centro recording, the amplitude of the later motions was not strongly affected. The 1968 El Centro displacement record (no. 5 in the figure) contains obvious surface-wave arrivals with dominant periods similar to the free period of the instrument; the instrument amplified this motion by about 80 per cent.

The Mt. Hamilton records are comparable to records of other smaller magnitude earthquakes so far as the duration of 5-sec period waves is concerned. The same can-

not be said for the peak motions since they were off-scale. Unfortunately, the theoretical motions are not much help without an independent constraint on the rupture velocity.

As suggested in Boore (1973), the details of the rupture process may make the ground motions near large faults quite variable, especially for motions with wavelengths smaller than the fault size. If true, it is difficult to say how the durations measured on the Mt. Hamilton records would compare to recordings from other magnitude 8 earthquakes at similar distances, or from recordings of the 1906 earthquake at other sites.

CONCLUSIONS

Although the location cannot be accurately determined, a main-shock epicenter in the vicinity of San Francisco is consistent with much of the data available for the earthquake: teleseismic data, $S - P$ and S times and relative amplitudes of S and P waves at Mt. Hamilton, the initial direction of motion in the duplex pendulum records at Mt. Hamilton and Berkeley, and the times at which various pendulum clocks stopped. The preferred epicenter near San Francisco agrees with Bolt's (1968) results. Although uncertain by at least $\pm \frac{1}{2}$ meter, the observed surface breakage (Figure 6) shows some interesting features, the foremost being the steplike nature of the curve and the decrease of the slip to the south. As suggested by Thatcher (1975), these features may be due to partial release of strain in these areas by the earthquakes of 1838, 1865, and 1890, which apparently occurred along the San Andreas fault to the south of San Francisco (*Report*, V. I, pp. 448-449). It is natural to suppose that the large change in slip from about $2\frac{1}{2}$ to over 4 m near San Andreas Lake marks the epicentral region of the main 1906 event. The results in this paper support this idea, but require that the epicenter be to the north of the change. Although the predominant part of the rupture was northwestward along the fault, the evidence suggests that southeastward rupture, if only over 10 km or so, must have been present. This part of the rupture would have little consequence for the radiation of long-period teleseismic waves.

The theoretical modeling showed that surface waves dominated the motion at Mt. Hamilton and also emphasized the sensitivity of the motions to directivity effects and rupture velocity. The general characteristics of the data (polarity, amplitude, period content, duration) were matched reasonably well by a simple dislocation model using fault lengths, depths, and offsets determined from independent data.

ACKNOWLEDGMENTS

Discussions with B. A. Bolt and T. V. McEvilly concerning the availability of data and the instruments on which they were recorded at Lick Observatory on Mt. Hamilton were helpful, as were discussions with H. Swanger and W. Joyner about the fault modeling. Thoughtful criticisms of the original manuscript were provided by A. G. Lindh and W. Thatcher. This research was supported by the Division of Earth Sciences, National Science Foundation, NSF Grant EAR76-02597, the Division of Advanced Environmental Research and Technology, National Science Foundation, Grant ENV75-05148, and by the U.S. Geological Survey, Contract 14053.

REFERENCES

- Aki, K. (1968). Seismic displacements near a fault, *J. Geophys. Res.* 73, 5359-5376.
 Anderson, J. G. (1976). Motions near a shallow rupturing fault: evaluation of effects due to the free surface, submitted to *Geophys. J.*
 Ben-Menahem, A. and S. J. Singh (1972). Computation of models of elastic dislocations in the earth, *Methods in Computational Physics*, Vol. 12, Bruce Bolt, Editor, Academic Press, New York, 229-375.

- Ben-Menahem, A., M. Rosenman, and D. G. Harkrider (1970). Fast evaluation of source parameters from isolated surface-wave signals, *Bull. Seism. Soc. Am.* **60**, 1337-1387.
- Boatwright, J. and D. M. Boore (1975). A simplification in the calculation of motions near a propagating dislocation, *Bull. Seism. Soc. Am.* **65**, 133-138.
- Bolt, B. A. (1968). The focus of the 1906 California earthquake, *Bull. Seism. Soc. Am.* **58**, 457-471.
- Bolt, B. A. (1973). Duration of strong ground motion, *Proc. World Conf. Earthquake Engr., 5th, Rome*, ppr. no. 292.
- Bolt, B. A., C. Lomnitz, and T. V. McEvilly (1968). Seismological evidence on the tectonics of central and northern California and the Mendocino escarpment, *Bull. Seism. Soc. Am.* **58**, 1725-1767.
- Boore, D. M. (1973). Empirical and theoretical study of near fault wave propagation, *Proc. World Conf. on Earthquake Engr., 5th, Rome*, ppr. no. 301a.
- Butler, R., H. Kanamori, and R. Geller (1975). Long-period ground motion in Los Angeles from a great earthquake on the San Andreas fault (abstract), *EOS, Trans. Am. Geophys. Union*, **52**, 1024.
- Cloud, W. K. and D. E. Hudson (1961). A simplified device for recording strong motion earthquakes, *Bull. Seism. Soc. Am.* **51**, 159-174.
- Dewey, J. and P. Byerley (1969). The early history of seismometry (to 1900), *Bull. Seism. Soc. Am.* **59**, 183-227.
- Ewing, J. A. (1881). On a new seismograph, *Proc. Roy. Soc. (London), Ser. A*, **31**, 440-446.
- Ewing, J. A. (1884a). Measuring earthquakes, I. Methods, *Nature* **30**, 149-152.
- Ewing, J. A. (1884b). Measuring earthquakes, II. Results, *Nature* **30**, 174-177.
- Ewing, J. A. (1885). A recent Japanese earthquake, *Nature* **31**, 581-582.
- Ewing, J. A. (1886). Earthquake recorders for use in observatories, *Nature* **34**, 343-344.
- Ewing, J. A. (1887). A recent Japanese earthquake, *Nature* **36**, 107-109.
- Harkrider, D. G. (1970). Surface waves in multilayered elastic media. Part II. Higher mode spectra and spectral ratios from point sources in plane-layered earth models, *Bull. Seism. Soc. Am.* **60**, 1937-1987.
- Helmberger, D. V. (1974). Generalized ray theory for shear dislocations, *Bull. Seism. Soc. Am.* **64**, 45-64.
- Holden, E. S. (1887). "Self-registering seismometers" in Description of the meteorological instruments, Ch. IX in *Publ. Lick Obs. of the Univ. of Calif.* **1**, 82-83.
- Kanamori, H. (1974). Long-period ground motion in the epicentral area of major earthquakes, *Tectonophysics* **21**, 341-356.
- Louderback, G. D. (1942). History of the University of California seismographic stations and related activities, *Bull. Seism. Soc. Am.* **32**, 205-229.
- Page, R. A., D. M. Boore, W. B. Joyner, and H. W. Coulter (1972). Ground motion values for use in the seismic design of the trans-Alaska pipeline system, *U.S. Geol. Surv. Circ.* **672**, 23 pp.
- Reid, H. F. (1910). *The Mechanics of the Earthquake*, Vol. II of *The California Earthquake of April 18, 1906*, Carnegie Institution of Washington (reprinted 1969), 192 pp.
- Savage, J. C. (1971). Radiation from supersonic faulting, *Bull. Seism. Soc. Am.* **61**, 1009-1012.
- Thatcher, W. (1975). Strain accumulation and release mechanism of the 1906 San Francisco earthquake, *J. Geophys. Res.* **80**, 4862-4872.

GEOPHYSICS DEPARTMENT
STANFORD UNIVERSITY
STANFORD, CALIFORNIA 94305

Manuscript received October 12, 1976